Modulation of the Kynurenine Pathway in Search for New Neuroprotective Agents. Synthesis and Preliminary Evaluation of (*m*-Nitrobenzoyl)alanine, a Potent Inhibitor of Kynurenine-3-hydroxylase

Roberto Pellicciari,* Benedetto Natalini, Gabriele Costantino, Mahmoud R. Mahmoud,† Luisa Mattoli, and Bahman M. Sadeghpour

Istituto di Chimica Farmaceutica e Tecnica Farmaceutica, Università di Perugia, Perugia, Italy

Flavio Moroni, Alberto Chiarugi, and Raffaella Carpenedo

Dipartimento di Farmacologia Preclinica e Clinica "Mario Aiazzi Mancini", Università di Firenze, Firenze, Italy

Received November 1, 1993®

The synthesis of (*o*-nitrobenzoyl)-, (*m*-nitrobenzoyl)-, and (*p*-nitrobenzoyl)alanine (*o*-, *m*-, and *p*-NBA), three new kynurenine analogues, and their evaluation as inhibitors of kynureninase and kynurenine-3-hydroxylase are reported. The most potent of these compounds, *m*-NBA, has an IC_{50} of $0.9 \pm 0.1\ \mu M$ as an inhibitor of kynurenine-3-hydroxylase and of $100 \pm 12\ \mu M$ as an inhibitor of kynureninase. When administered to rats, *m*-NBA significantly increases the concentration of kynurenine and kynurenic acid in the brain as well as in blood and in the liver. *m*-NBA has also been shown to increase the concentration of kynurenic acid in hippocampal extracellular fluid. This increase is associated with sedative and anticonvulsant activities, thus confirming the possibility of antagonizing L-glutamate-mediated effects by modulating the kynurenine pathway of L-tryptophan metabolism.

Introduction

Unachieved in a clinically useful way, pharmacological control of the central nervous system (CNS) excitatory pathways responding to the neurotransmitter L-glutamate is an exceedingly important goal.[1] Indeed, an abnormally intense exposure to L-Glu has been implicated in the pathogenesis of several neurological disorders either chronic (Alzheimer's, Parkinson's, amyotrophic lateral sclerosis, etc.) or caused by acute insult (hypoxia/ischemia, hypoglycaemia, head trauma, etc.). Among the strategies aimed at reducing the overstimulation of the glutamatergic receptors, the modulation of the L-kynurenine (KYN) catabolic pathway of L-tryptophan (L-Trp) in the brain (Scheme 1) is gaining considerable interest since the discovery that two metabolites along the route, kynurenic acid (KYNA) and quinolinic acid (QUIN), interact with the *N*-methyl-D-aspartate (NMDA) receptor complex in a functionally opposite manner.[2] KYNA is a nonselective antagonist at the strychnine-insensitive glycine recognition site and is endowed with neuroprotective properties,[3] whereas QUIN, a selective agonist at the NMDA site of the NMDA receptor complex, is a relatively potent neurotoxin which has been implicated in the pathogenesis of a variety of neurological disorders, including Huntington's disease.[4] Increased concentrations of QUIN have also been indicated as responsible for neurological disturbances accompanying many infections and inflammatory diseases, including acquired immune deficiency syndrome (AIDS).[41] Recently, Heyes et al. have also reported that a delayed increase in the level of QUIN occurs in several brain regions following transient ischemia.[5]

Two main strategies aimed at favorably altering the KYNA/QUIN balance have so far been followed, the first one focused on the development of more selective and

Scheme 1

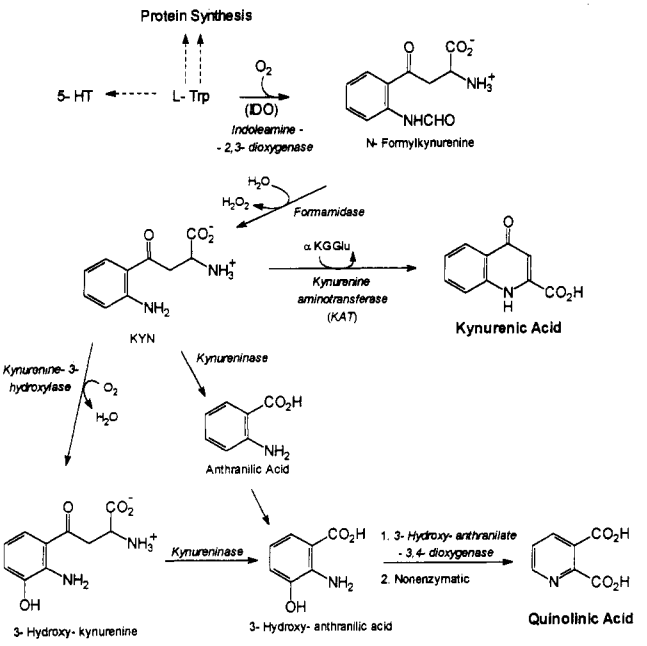

potent KYNA analogues,[6] and a second one aimed either at blocking QUIN's production or at increasing the KYNA production by inhibiting key enzymes of the KYN pathway, a task facilitated by the recent advances in the elucidation of its physiology and biochemistry. Here are some relevant points: (a) The KYN pathway is mainly localized in systemic tissues, especially the liver, while most of L-Trp in the CNS is converted to indolamines or utilized in protein synthesis.[7] (b) Neither QUIN nor KYNA can enter the brain due to their polar nature and the lack of active transport mechanism.[8] (c) KYN can readily cross the blood-brain barrier by using a neutral amino acid transporter[9] and is the main source of KYNA in normal brain by the action of KYN aminotransferase, an enzyme preferentially localized in astrocytes but also

† On leave from Department of Chemistry, Ain Shams University, Cairo, Egypt.

® Abstract published in *Advance ACS Abstracts*, February 1, 1994.

0022-2623/94/1837-0647$04.50/0

present in neurons,[10] which may significantly increase the production of KYNA[3g,11] and its accumulation in the brain when more KYN is available. (d) There is an apparent inability of normal brain to convert either L-Trp or KYN to QUIN. The only QUIN precursor in normal brain, 3-hydroxyanthranilate, is converted to QUIN by the action of 3-hydroxyanthranilic acid oxygenase (3-HAO), which is present in the astrocytes surrounding glutamatergic synapses.[12] The *de novo* conversion in the brain of L-Trp to QUIN has been demonstrated to occur only following transient cerebral ischemia probably as a consequence of the presence of macrophage infiltrates with their KYN biosynthetic machinery in damaged brain regions.[5] (e) An increase in the concentration of KYNA, which is normally relatively low in brain tissues (ca. 0.1 μM),[3d,13] leads to the manifestation of pharmacological effects compatible with antagonist activity toward EAA receptors.[14] In inhibitor design, most efforts have so far been focused on two enzymes of the KYN pathway, indolamine-2,3-dioxygenase (IDO)[15] and kynureninase. In this connection, a recent paper by Phillips et al.[16] reporting the design and synthesis of *S*-aryl-L-cysteine *S*,*S*-dioxide derivatives as selective and potent inhibitors of kynureninase is particularly relevant.

We have reported, previously, that nicotinoylalanine (NAL, **1**), a KYN analog hypothesized to interfere with kynureninase and kynurenine-3-hydroxylase, increases the concentration of KYNA in brain tissues and has *in vivo* anticonvulsant activity, albeit at high doses.[17] In view of the interesting biological properties exhibited by NAL, and also in order to assess the role played by each of the two enzymes in this activity, we have pursued a program aimed at developing KYN analogues more potent and selective than **1**. Here we report that one of the compounds that we have prepared, (*m*-nitrobenzoyl)alanine (*m*-NBA, **4b**), is the first potent and selective competitive inhibitor of kynurenine-3-hydroxylase so far reported. *In vivo*, xanthurenic acid has been reported to exert a feedback control on the concentration of 3-hydroxykynurenine and KYN by inhibiting kynurenine-3-hydroxylase.[18] A comparison between *m*-NBA (**4b**) and NAL (**1**) as inhibitors of kynureninase and kynurenine-3-hydroxylase as well as the activity of *m*-NBA (**4b**) in preventing seizures induced by maximal electroshock in rats or by acoustic stimulation in DBA-2 mice are also reported herein.

Chemistry

The synthesis of NAL (**1**) was carried out according to previously reported methods.[17c] The synthesis of (±) (*o*-nitrobenzoyl)alanine (*o*-NBA, **4a**) begins with the condensation of *o*-nitrophenacyl bromide (**2a**) with diethyl sodioacetamidomalonate in DMF at room temperature for 5 h to afford, after recrystallization, diethyl (*o*-nitrophenacyl)acetamidomalonate (**3a**) in 33% yield. Hydrolysis of **3a** with 6 N HCl followed by neutralization with sodium hydrogen carbonate afforded *o*-NBA (**4a**) as a free base in 65% yield. Analogously, starting from *m*-nitrophenacyl bromide (**2b**) and *p*-nitrophenacyl bromide (**2c**), (*m*-nitrobenzoyl)alanine (*m*-NBA, **4b**) and (*p*-nitrobenzoyl)alanine (*p*-NBA, **4c**) were obtained as free bases in 28.5 and 22% overall yield, respectively (Chart 1).

Chart 1

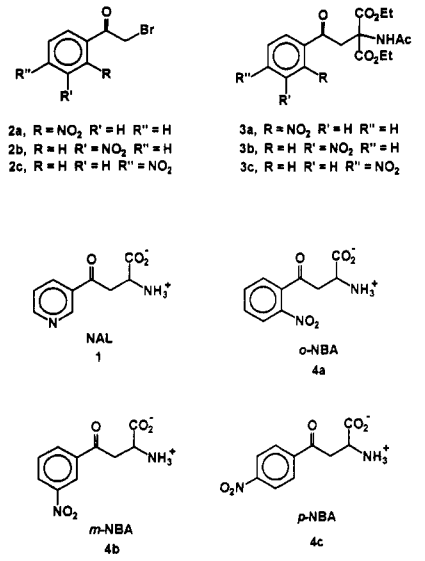

Table 1. Competitive Inhibition Assay (μM)

compound	IC_{50} kynureninase	IC_{50} kynurenine-3-hydroxylase
NAL (1)	800 ± 120	900 ± 180
o-NBA (**4a**)	100 ± 12	2000 ± 200
m-NBA (**4b**)	100 ± 12	0.9 ● 0.1
p-NBA (**4c**)	900 ± 120	300 ± 60

Table 2. Effect of *m*-NBA (**4b**, 400 mg/kg ip) on the Content of KYN and KYNA in Rat Organs[a]

	KYN		KYNA	
	saline	*m*-NBA	saline	*m*-NBA
brain	300 ± 20	4000 ± 350*	30 ± 5	150 ± 30*
liver	660 ± 70	4000 ± 450*	70 ± 14	250 ± 22*
blood	3000 ± 280	16000 ± 1200*	50 ± 10	120 ± 29*

[a] Values are expressed in picomoles/gram of tissue and are the mean ± SEM of at least five determinations. Statistical differences were evaluated according to ANOVA and Dunnett's *t* test[30] for grouped data. *$p < 0.01$ versus saline.

Results and Discussion

Inhibition. The results of competitive inhibition studies are shown in Table 1. The IC_{50}'s for **1** and **4a–c** were obtained by utilizing the experimental setting reported in Figure 1, where the dose–response curves of these inhibitors were obtained by using a single concentration (100 μM) of substrate. *p*-NBA (**4c**) exhibited an IC_{50} of 900 ± 120 μM for kynureninase and 300 ± 60 μM for kynurenine-3-hydroxylase, thus showing relatively low potency and selectivity. *m*-NBA (**4b**), with an IC_{50} of 0.9 ± 0.1 μM for kynurenine-3-hydroxylase and 100 ± 12 μM for kynureninase, resulted a potent and selective inhibitor toward the former enzyme. *o*-NBA (**4a**), on the other hand, exhibited an opposite profile, having an IC_{50} of 100 ± 12 μM for kynureninase and 2000 μM for kynurenine-3-hydroxylase.

NAL (**1**), with an IC_{50} of 800 ± 120 μM for kynureninase and 900 ± 180 μM for kynurenine-3-hydroxylase, showed similar but weak activities toward both enzymes.

Effect of *m*-NBA (4b) on KYN and KYNA Content in the Brain and Other Organs of the Rat. The administration of *m*-NBA (**4b**, 400 mg/kg ip) significantly increased the content of both KYN and KYNA in the brain (Table 2). In the whole brain KYN concentration increased 13 times and KYNA concentration increased

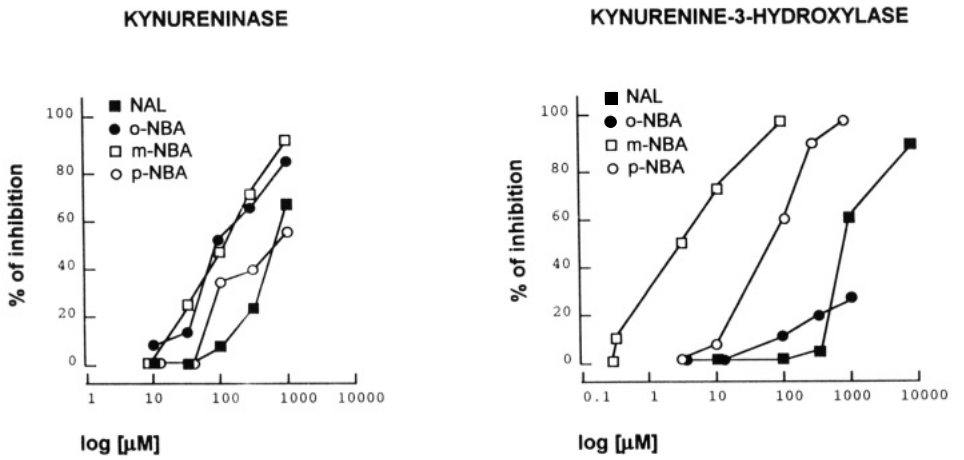

Figure 1. Inhibition of kynureninase and kynurenine-3-hydroxylase by *o*-NBA (**4a**), *m*-NBA (**4b**), *p*-NBA (**4c**), and NAL (**1**). Different concentrations of inhibitors were used while the substrate was 100 μM. Each point represents the mean of at least four different experiments, each performed in duplicate. Standard errors were within 10%.

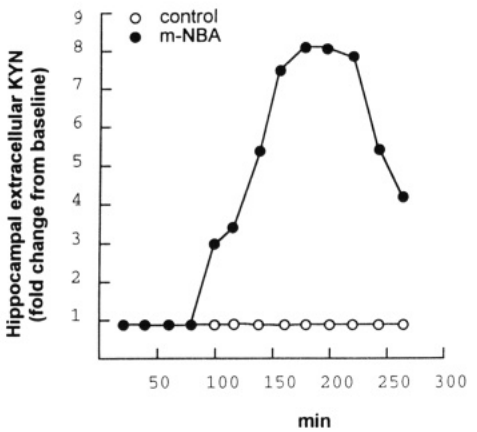

Figure 2. Effects of *m*-NBA (**4b**) 200 mg/kg ip on KYN concentrations in the rat hippocampal dialysate. Data are the average of five rats and are expressed as changes from the baseline value (0.1 ± 0.004 μM). Standard errors were within 15%.

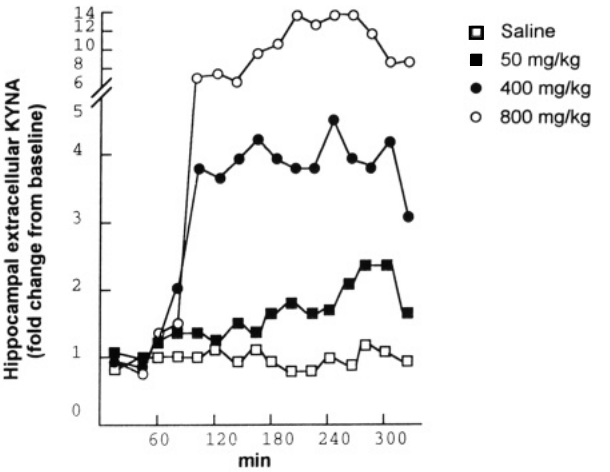

Figure 3. Effect of different doses of *m*-NBA (**4b**) on KYNA concentration in rat hippocampal dialysate. Data are average values of at least five rats per each dose. Standard errors were within 20% of the reported values. The basal concentration of KYNA (found after 1.5 h of perfusion) in the microdialysis perfusate was 11.5 ± 0.8 μM (mean ± SEM of 400 determinations) and was relatively stable up to 12 h of perfusion.

up to 5 times. The administration of *m*-NBA (**4b**) was also shown to increase significantly the extracellular concentration of KYNA.

Effects of *m*-NBA (4b) on the Extracellular Concentration of KYN and KYNA in the Rat Hippocampus. *m*-NBA (**4b**, 200 mg/kg ip) significantly increased the extracellular concentration of KYN. The increase developed after 1 h of *m*-NBA (**4b**) administration and produced the maximum content of KYN within 3 h (Figure 2). Similarly, the extracellular concentration of the excitatory amino acid antagonist KYNA significantly increased after administration of different doses of *m*-NBA (Figure 3).

Sedative and Anticonvulsant Effects of *m*-NBA (4b). Rats injected with *m*-NBA (**4b**) appeared relatively calm and easy to manage. Moreover, *m*-NBA (**4b**) significantly decreased the spontaneous locomotor activity in a dose-dependent manner (Figure 4). Analogous doses of *m*-NBA (**4b**) reduced the total duration (tonic and clonic component) of maximal electroshock-induced seizures (Figure 5). When tested in DBA-2 mice, *m*-NBA (**4b**) completely antagonized both the tonic and clonic component of the seizures induced by acoustic stimulation (Table 3).

The present results give support to a series of hypotheses, the first of which is the therapeutic potential harbored in the adjustment of KYNA or QUIN as a novel strategy for

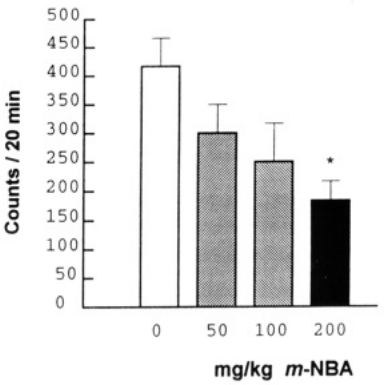

Figure 4. Effect of *m*-NBA (**4b**) at the reported doses on spontaneous locomotor activity of rats. Each rat was placed in a clean cage for 20 min starting 2.5 h after *m*-NBA administration. Each column was obtained by averaging the number of interruptions of photocells with five different rats. Vertical bars are SEM. $*p < 0.05$ versus saline according to ANOVA and Dunnett's *t* test.[30]

the treatment of neurological diseases, including neurodegenerative diseases and convulsive states. Also confirmed is the importance of increasing the brain concen-

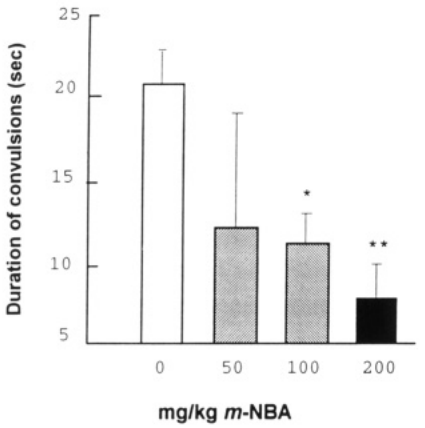

Figure 5. Effect of *m*-NBA (**4b**) on the duration of convulsions induced by maximal electroshock. *m*-NBA was administered 2.5 h before the test at the reported doses. Data are mean ± SEM (bars) of groups of at least 10 animals. $*p < 0.05$ and $**p < 0.01$ versus saline according to ANOVA and Dunnett's *t* test.[30]

Table 3. Effect of *m*-NBA (**4b**) on Sound-Induced Convulsions in DBA-2 Mice[a]

		convulsions		
		clonic	tonic	death
saline		13/15	9/15	5/15
m-NBA	200 mg/kg ip	4/6	2/6	2/6
	400 mg/kg ip	6/13**	1/13*	0/13

[a] *m*-NBA (**4b**) was dissolved in saline and administered 2 h before the acoustic stimulation. $*p < 0.05$, $**p < 0.01$ by χ^2 test compared with saline.

tration of KYNA. Thus, it is possible to relate the decrease of spontaneous motor activity (Figure 4) and the decrease of the duration of convulsions (Figure 5) observed after treatment with *m*-NBA (**4b**) to the increase of KYNA levels in brain extracellular spaces. It should be pointed out, in this connection, that these behavioral effects are analogous to those elicited by the administration of excitatory amino acid receptor antagonists and, among these, by antagonists of the glycine site of the NMDA receptor complex, to which class KYNA belongs. The observed elevation of KYNA brain levels, in turn, is a consequence of the increase of KYN in liver, blood, brain, and hippocampal extracellular spaces obtained by inhibiting both kynureninase and kynurenine-3-hydroxylase in the case of NAL (**1**), and mainly the latter enzyme in the case of *m*-NBA (**4b**). The experiments here described do not give information on the site of action of NAL (**1**) and *m*-NBA (**4b**). This site should not necessarily be in the brain, since the increase at the central level of KYN availability as a consequence of the peripheral inhibition of KYN pathway is probably sufficient to explain the observed increase of KYN production in the CNS. The ability of *m*-NBA (**4b**) to antagonize QUIN biosynthesis is under investigation.

Mechanism of Kynurenine-3-hydroxylase Inhibition. Molecular Modeling Study. Kynurenine-3-hydroxylase (EC 1.14.13.9) is an external flavoprotein monoxygenase located in the outer mitochondrial membrane, which incorporates oxygen into KYN to give 3-hydroxykynurenine and requires FAD as a cofactor and either NADH or NADPH as coreductant.[19] A possible representation of the full catalytic cycle of kynurenine-3-hydroxylase useful as a working hypothesis, based on available kinetic and spectroscopic data[19,20] and on the strict analogies existing with the well-studied flavoprotein phenolic hydroxylases,[21,22] is presented in Scheme 2. The scheme begins with a reduced enzyme/KYN complex which reacts with molecular oxygen (intermediate **I**) to give the corresponding C(4a)-hydroperoxyflavin intermediate **II** (step a). Electrophilic attack from the hydroperoxy group to the aromatic ring of KYN (step b), followed by electron-transfer reaction (step c), deprotonation of the cationic substrate, and concomitant protonation of isoalloxazine anionic group[22] (step d) leads to intermediate **V** which undergoes dehydration of the hydroxyflavin moiety and liberation of 3-hydroxykynurenine (step e). A new molecule of KYN binds then to the enzyme, and the catalytic cycle is completed when the enzyme/KYN complex binds to NADPH, the flavin is reduced again, and $NADP^+$ is liberated.

It may be assumed that the inhibitory activity exerted by *m*-NBA (**4b**) toward kynurenine-3-hydroxylase and, in particular, its high potency and selectivity with respect to *o*-NBA (**4a**) and *p*-NBA (**4c**) as well as to NAL (**1**) are related to stereoelectronic features favoring its binding to the active site of the enzyme. In order to assess the plausibility of this assertion, molecular modeling studies have been carried out. In the absence of experimental data concerning the conformation of the enzyme-bound ligands, we have initially considered them as having their side chain in the energetically favored extended conformation. As a model for the tridimensional structure of the active site, moreover, it was decided to construct an explicit molecular framework around the ligands able to account for primary interactions between the ligands and the macromolecule. This approach can permit the disclosure of possible correlations between the inhibitory activities and the calculated interaction energies, which account for the binding potency. This procedure is closely related to the "pseudoreceptor approach",[23] a method successfully utilized for the evaluation of ligands acting at membrane-bound receptors and for the calculation, in a semiquantitative way, of the observed free energies of binding.[24] In the present case, we have constructed a "pseudoactive site" around KYN as follows. Putative binding sites on the active site were identified by using GRID,[25] a program which evaluates noncovalent interactions between a molecule and a variety of possible chemical probes moving around the molecule. The tridimensional regions corresponding to the most favorable interaction energy can thus be taken as the location of the binding points on the active site. In the present case three probes have been used, namely a cationic sp^3 NH group, a carboxylate group, and a phenolic OH group, simulating positively charged, negatively charged, and hydrogen bonding donor/acceptor active-site residues, respectively. Once the GRID energy contour maps were generated, the regions of favorable interaction were adequately accommodated by surrounding the substrate with lysine, aspartate, and tyrosine fragments. These fragments were then linked together by hydrocarbon spacers, and the resulting complex was geometry optimized with molecular mechanics. In a separate operation, the complex formed by the interaction of the reduced isoalloxazine moiety of FAD and molecular oxygen (intermediate I, Scheme 2) was optimized by utilizing a semiempirical method (PM3/MOPAC).[26] The two superstructures thus obtained (pseudoactive site/KYN and isoalloxazine/O_2) were then combined together to give a complex in which the molecular oxygen is directed toward position 3 of KYN and further geometry optimized. The resulting structure showed, as

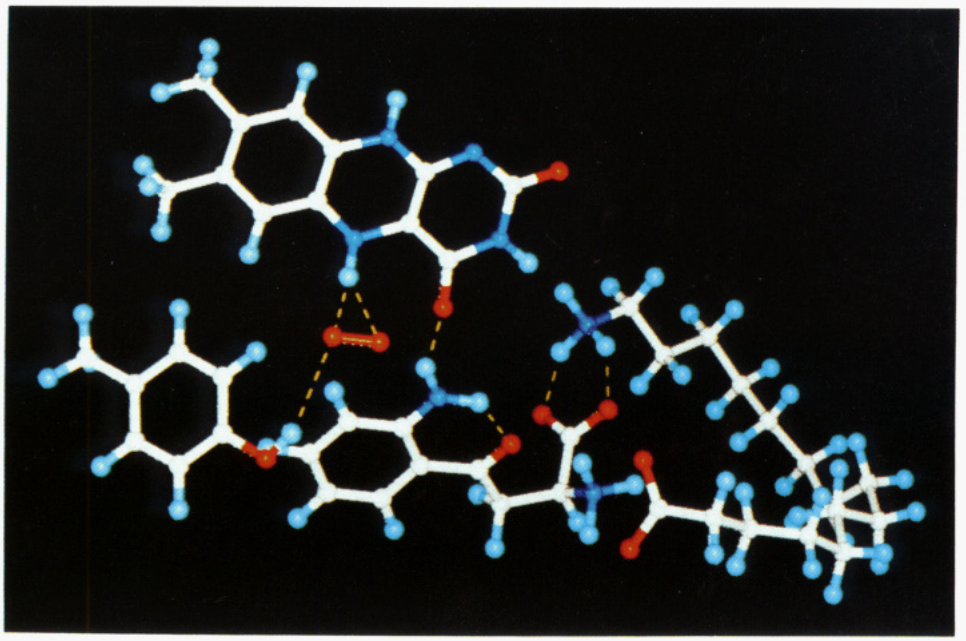

Figure 6. Geometry-optimized complex arising from the combination of two superstructures, pseudoactive site–KYN and isoalloxazine–O_2, and showing a hydrogen bond network among KYN, O_2, isoalloxazine, and the proteic portion.

Scheme 2

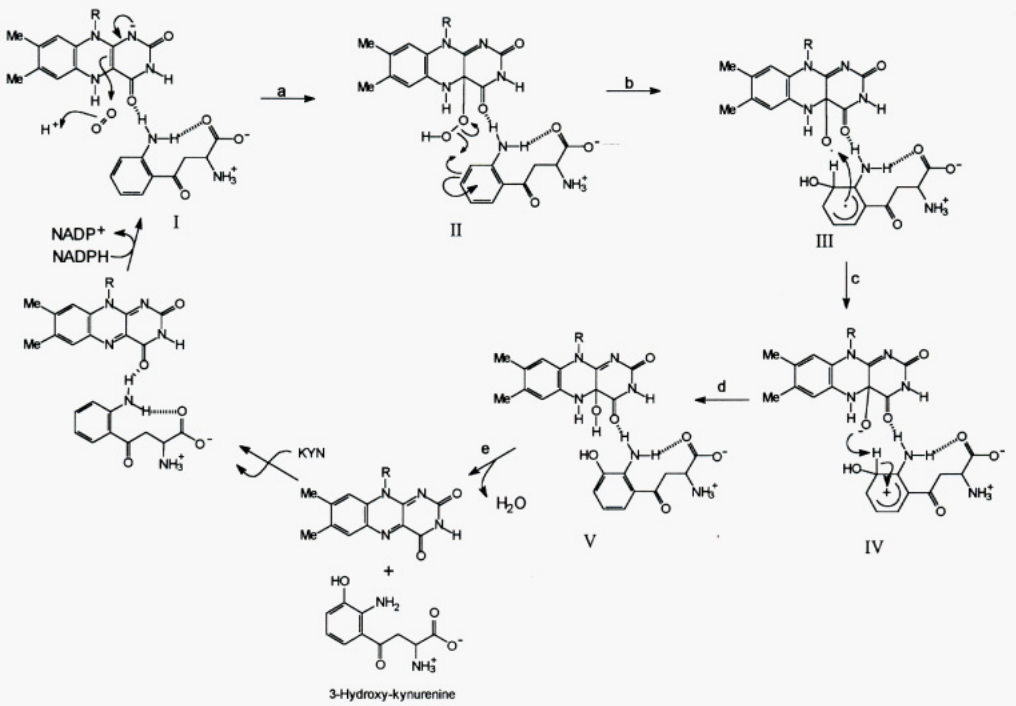

expected, a hydrogen-bond network among KYN, O_2, isoalloxazine, and the proteic portion (Figure 6). In order to prove whether this tridimensional model could account for the observed affinity of the ligands, the molecular oxygen was removed from the complex and KYN was substituted, in separate operations, by NAL (**1**), *m*-NBA (**4b**), *p*-NBA (**4c**), and *o*-NBA (**4a**). When *m*-NBA (**4b**) was allowed to relax within the complex, it was shown to adopt a disposition strictly resembling that of KYN (Figure 7a). In particular, one of the oxygen atoms of the nitro group was shown to mimic closely the oxygen atom of molecular oxygen involved in the hydrogen-bonding network. None of the other ligands was able to adopt a similar disposition (Figure 7b–d). While the weak affinity of NAL (**1**) for kynurenine-3-hydroxylase may be attributed to the lack of an oxygen mimicking group (and therefore to the lack of part of the hydrogen bonding network), for the *o*-NBA (**4a**) and *p*-NBA (**4c**) the weak affinity probably derives from an unfavorable orientation of the oxygen atoms of the nitro group and/or from the occupation of a forbidden steric region. The relative interaction energies between the various ligand and the pseudoactive site are reported in Table 4. These energies have been calculated by evaluating the energy of the ligand, of the active site and of the pseudoactive site–ligand complex. The difference between the sum of the first two terms and the third can be seen as an estimation of the interaction energy of that ligand and the pseudoactive site. Even if these energies are not free energies and therefore cannot be directly compared with affinity data,

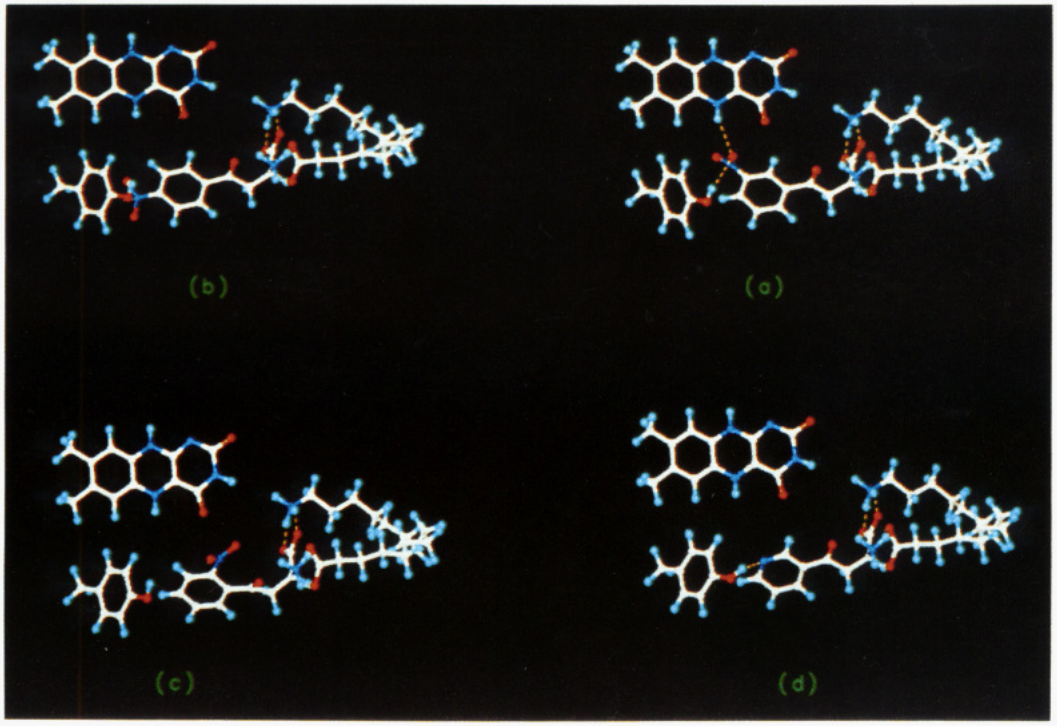

Figure 7. Geometry-optimized complex obtained as a result of the substitution of both KYN and O_2, as previously shown (Figure 6) with *m*-NBA (a), *p*-NBA (b), *o*-NBA (c), and NAL (d), respectively.

Table 4. Molecular Mechanics Interaction Energies between Ligands and the Pseudoactive Site

compound	$\Delta E^{a,b}$	$-\log(IC_{50}^*/IC_{50})^c$
m-NBA (**4b**)	0.0	0.0
p-NBA (**4c**)	1.3	2.52
NAL (**1**)	1.9	2.89
o-NBA (**4a**)	4.3	2.94

[a] Energy in kilocalories/mole. [b] Differences in interaction energy between *m*-NBA (**4b**) and the other ligands. [c] Differences (as logarithms) between IC_{50} (IC_{50}^*) of *m*-NBA and IC_{50}'s of the other ligands.

the qualitative correlation found among them may be considered as a clue useful for more advanced studies on the molecular mechanisms underlying the inhibition of kynurenine-3-hydroxylase.

Conclusion

This study reports the synthesis and preliminary biological evaluation of (*m*-nitrobenzoyl)alanine (*m*-NBA, **4b**), the most powerful and selective inhibitor of kynurenine-3-hydroxylase reported to date. *m*-NBA (**4b**), which is 1000 times more active than the previously reported NAL (**1**) and by far more selective, is an useful tool for further characterizing kynurenine-3-hydroxylase. Also, in view of the anticonvulsant activity exhibited, **4b** may represent a valuable candidate for further therapeutic investigations. Experiments along these lines are in progress in our laboratories and will be detailed in future reports.

Experimental Section

General Methods. Melting points were determined on a Kofler micro-hot-stage apparatus and are uncorrected. IR spectra were recorded with a Perkin-Elmer 1320 spectrometer. ^{1}H-NMR and ^{13}C-NMR spectra were taken on a Bruker AC 200 spectrometer, and the chemical shifts are in ppm downfield from tetramethylsilane, except in the presence of D_2O which was also used as internal standard. GC–mass spectrometry was performed on a Hewlett-Packard gas chromatograph HP 5890 (column and conditions: HP-1, 12 m, 0.2-mm i.d., 0.33-μm ft, 150(1′)/280 °C, 10 °C/min) equipped with a mass detector HP 5971. Flash chromatography was performed on Merck silica gel (0.040–0.063 mm).

Diethyl (*o*-Nitrophenacyl)acetamidomalonate (3a). Sodium hydride (0.916 g, 22.95 mmol, from a 60% mineral oil suspension) was added to a magnetically stirred solution of diethyl acetamidomalonate (4.98 g, 22.95 mmol) in anhydrous DMF (30 mL) at room temperature in a nitrogen atmosphere. Stirring was continued for 3 h after which a solution of *o*-nitrophenacyl bromide (**2a**, 5.0 g, 20.49 mmol) in anhydrous DMF (9 mL) was added dropwise over 20 min, and the resulting dark red mixture was kept with stirring for 5 h. The reaction mixture was then poured into water (300 mL) and, after acidification with 3 N HCl, was extracted with ether (5 × 60 mL). The combined organic phases were washed with brine (100 mL) and dried over anhydrous sodium sulfate. Evaporation of the solvent gave a residue (7.5 g) which was triturated with ether (200 mL) and recrystallized from ether/dichloromethane (3:1) to give **3a** (2.6 g, 33%): mp 121–2 °C; IR ($CHCl_3$) ν_{max} 1700, 1540, 1500, 1360, 1310 cm^{-1}; ^{1}H-NMR ($CDCl_3$) δ 1.30 (6H, t, 2 × CH_2CH_3), 2.10 (3H, s, $COCH_3$), 4.15 (2H, s, 3-CH_2), 4.30 (4H, dd, 2 × CH_2CH_3), 7.15 (1H, br s, NH), 7.40 (1H, d, J = 7 Hz, 6′-CH), 7.60 (1H, t, J = 7 Hz, 5′-CH), 7.70 (1H, t, J = 7 Hz, 4′-CH), 8.10 (1H, d, J = 7 Hz, 3′-CH); ^{13}C-NMR ($CDCl_3$) δ 13.76, 22.79, 45.52, 62.92, 63.51, 124.44, 127.12, 130.87, 133.89, 136.23, 145.68, 166.69, 169.62, 198.77; GC-MS 307 (5.5), 265 (21.89), 219 (4.14), 150 (100). Anal. ($C_{17}H_{20}N_2O_8$) C, H, N.

(*o*-Nitrobenzoyl)alanine (4a). A suspension of **3a** (1.00 g, 2.63 mmol) in 6 N HCl (25 mL) was refluxed for 5 h. After cooling, the reaction mixture was washed with ethyl acetate (2 × 5 mL) and concentrated under reduced pressure to give an oily residue (0.65 g) which after trituration with acetone yielded the pure hydrochloride salt (0.475 g, 66%), mp 196–7 °C dec. An aqueous solution of this salt was then neutralized with 5% sodium hydrogen carbonate solution to afford the free base **4a** (0.41 g, 99% from the salt): mp 189–90 °C dec; IR (KBr) ν_{max} 1700, 1535, 1485, 1360, 1310; ^{1}H-NMR (D_2O + CD_3OD + CF_3CO_2H) δ 3.14 (2H, d, 3-CH_2), 4.00 (1H, t, 2-CH), 7.00 (1H, d, J = 7 Hz, 6′-CH), 7.20 (1H, t, J = 7 Hz, 5′-CH), 7.30 (1H, t, J = 7 Hz, 4′-CH), 7.60 (1H, d, J = 7 Hz, 3′-CH); ^{13}C-NMR (D_2O + CD_3OD + CF_3CO_2H) δ 42.60, 49.44, 125.63, 128.50, 133.03, 135.45, 136.04, 146.11, 171.33, 201.76. Anal. ($C_{10}H_{10}N_2O_5$) C, H, N.

Diethyl (*m*-Nitrophenacyl)acetamidomalonate (3b). So-

dium hydride (1.90 g, 47.5 mmol, from a 60% mineral oil suspension) was added to a magnetically stirred solution of diethyl acetamidomalonate (10.0 g, 46.03 mmol) in anhydrous DMF (38 mL) at room temperature in a nitrogen atmosphere. Stirring was continued for 3 h after which a solution of *m*-nitrophenacyl bromide (**2b**, 10.0 g, 41.0 mmol) in anhydrous DMF (27 mL) was added dropwise over 20 min, and the resulting dark red mixture was kept with stirring for 5 h. The reaction mixture was then poured into water (500 mL) and, after acidification with 3 N HCl, extracted with ethyl acetate (5 × 200 mL). The combined organic phases were washed with brine (100 mL) and dried over anhydrous sodium sulfate. Evaporation of the solvent gave an oily residue (17 g) which was submitted to flash chromatography: elution with petroleum ether–ethyl acetate (7:3) afforded a solid which was further purified by recrystallization with diethyl ether to give **3b** (5.0 g, 32%): mp 120–1 °C; IR ($CHCl_3$) ν_{max} 1700, 1540, 1500, 1360, 1310 cm^{-1}; ^1H-NMR ($CDCl_3$) δ 1.30 (6H, t, 2 × CH_2CH_3), 2.00 (3H, s, $COCH_3$), 4.20–4.40 (6H, m, 2 × CH_2CH_3 and 3-CH_2), 7.15 (1H, br s, NH), 7.70 (1H, t, J = 8 Hz, 5′-CH), 8.40 (2H, dd, J = 8 Hz, 4′-CH and 6′-CH), 8.80 (1H, d, J = 2 Hz, 2′-CH); ^{13}C-NMR ($CDCl_3$) δ 13.71, 22.69, 42.29, 62.84, 63.83, 122.80, 127.36, 127.54, 133.53, 137.26, 148.47, 166.75, 169.54, 194.72; GC–MS 380 (M^+, 1.1), 265 (51.79), 219 (31.90), 150 (100). Anal. ($C_{17}H_{20}N_2O_8$) C, H, N.

(*m*-Nitrobenzoyl)alanine (4b). A suspension of **3b** (7.30 g, 19.19 mmol) in 6 N HCl (100 mL) was refluxed for 10 h. After cooling, the reaction mixture was washed with ethyl acetate (2 × 30 mL) and concentrated under reduced pressure to give an oily residue (5.5 g) which after trituration with acetone yielded the pure hydrochloride salt (4.75 g, 90%), mp 180–181 °C dec. An aqueous solution of this salt was then neutralized with 5% sodium hydrogen carbonate solution to afford the free base **4b** (4.11 g, 99.5% from the salt): mp 187–8 °C dec; IR (KBr) ν_{max} 1700, 1535, 1485, 1360, 1310; ^1H-NMR (D_2O + CD_3OD + CF_3CO_2H) δ 3.25 (2H, d, 3-CH_2), 3.90 (1H, t, 2-CH), 7.05 (1H, t, J = 8 Hz, 5′-CH), 7.70 (2H, t, J = 8 Hz, 4′- and 6′-CH), 8.10 (1H, s, 2′-CH); ^{13}C-NMR (D_2O + CD_3OD + CF_3CO_2H) δ 39.27, 49.83, 123.82, 129.43, 131.48, 135.25, 137.25, 149.26, 171.67, 197.36. Anal. ($C_{10}H_{10}N_2O_5$) C, H, N.

Diethyl (*p*-Nitrophenacyl)acetamidomalonate (3c). Sodium hydride (1.90 g, 47.5 mmol, from a 60% mineral oil suspension) was added to a magnetically stirred solution of diethyl acetamidomalonate (9.97 g, 45.9 mmol) in anhydrous DMF (38 mL) at room temperature in a nitrogen atmosphere. Stirring was continued for 3 h, after which a solution of *p*-nitrophenacyl bromide (**2c**, 10.0 g, 41.0 mmol) in anhydrous DMF (27 mL) was added dropwise over 20 min, and the resulting dark red mixture was kept with stirring for 5 h. The reaction mixture was then poured into water (500 mL) and, after acidification with 3 N HCl, was extracted with ethyl acetate (5 × 200 mL). The combined organic phases were washed with brine (100 mL) and dried over anhydrous sodium sulfate. Evaporation of the solvent gave an oily residue (17 g) which was submitted to flash chromatography: elution with petroleum ether–ethyl acetate (8:2) afforded **3c** (5.0 g, 32%): mp 111–2 °C; IR ($CHCl_3$) ν_{max} 1700, 1535, 1500, 1350, 1310; ^1H-NMR ($CDCl_3$) δ 1.30 (6H, t, 2 × CH_2CH_3), 2.00 (3H, s, $COCH_3$), 4.20–4.40 (6H, m, 2 × CH_2CH_3 and 3-CH_2), 7.20 (1H, br s, NH), 8.20 (4H, dd, J = 9 Hz, aromatics); ^{13}C-NMR ($CDCl_3$) δ 13.76, 22.76, 42.50, 62.95, 63.81, 123.81, 129.88, 140.32, 150.48, 166.77, 169.60, 195.46; GC–MS 380 (M^+, 1.17), 265 (51.79), 219 (29.96), 150 (100). Anal. ($C_{17}H_{20}N_2O_8$) C, H, N.

(*p*-Nitrobenzoyl)alanine (4c). A suspension of **3c** (4.0 g, 10.5 mmol) in 6 N HCl (100 mL) was refluxed for 9 h. After cooling, the reaction mixture was washed with ethyl acetate (2 × 20 mL) and concentrated under reduced pressure to give an oily residue (3 g) which after trituration with acetone yielded the pure hydrochloride salt (2.0 g, 70%), mp 171–2 °C dec. An aqueous solution of this salt was then neutralized with 5% sodium hydrogen carbonate solution to afford the free base **4c** (1.73 g, 99.5% from the salt): mp 178–9 °C dec; IR (KBr) ν_{max} 1695, 1535, 1490, 1360, 1310 cm^{-1}; ^1H-NMR (D_2O + CD_3OD + CF_3CO_2H) δ 3.10 (2H, d, 3-CH_2), 3.80 (1H, t, 2-CH), 7.40 (4H, dd, J = 9 Hz, aromatics); ^{13}C-NMR (D_2O + CD_3OD + CF_3CO_2H) δ 39.48, 49.44, 124.84, 130.39, 140.76, 151.82, 171.56, 198.03. Anal. ($C_{10}H_{10}N_2O_5$) C, H, N.

Biological Tests. Evaluation of Enzyme Activity. Kynurenine-3-hydroxylase activity was evaluated in brain and liver by monitoring the formation of 3-hydroxykynurenine in tissue homogenates incubated in the presence of different concentration of KYN. The tissues were homogenized in 8 volumes of ice-cold 0.32 M sucrose and centrifuged at 4 °C for 30 min at 10000*g*. The pellets were washed two times by suspension and centrifugation in sucrose and, finally, suspended in 10–15 volumes of 0.14 M KCl/20 mM potassium phosphate buffer pH 7. The reaction mixture consisted of 50 μL of suspended pellet and 100 μL of phosphate buffer solution (100 mM, pH 7.5) containing 4 mM $MgCl_2$, different concentrations of KYN, and 4 mM NADPH. After 5–30 min of incubation at 37 °C, the reaction was terminated by addition of 0.1 mL of 20% (wt/vol) trichloroacetic acid. Kynureninase was monitored by measuring the formation of anthranilic acid in brain or liver homogenates incubated in the presence of KYN. Briefly, the tissues were homogenized in phosphate buffer (20 mM, pH 7) containing KCl (140 mM). The supernatants obtained after centrifugation (20000*g* for 30 min at 4 °C) were directly used as enzyme source. The reaction mixture consisted of 50 μL of this supernatant and 50 μL of substrate solution containing 200 mM Tris-HCl buffer pH 8, 100 μM pyridoxal phosphate, and different concentration of KYN. After a 30-min incubation at 37 °C, the reaction was terminated by adding 0.1 mL of 20% (wt/vol) trichloroacetic acid.

Implantation of the Dialysis Membrane. The experiments in rodents were formally approved by an ethical committee and were performed according to the rules of the University of Firenze. Adult male Wistar rats (Morini, Reggio Emilia, Italy) weighing 180–220 g were used. They were anesthetized using chloral hydrate (300 mg/kg ip) and placed in a stereotaxic apparatus. The skull was opened. A transcerebral microdialysis probe (AN 69 membrane, Dasco, Italy; 220-μm internal diameter; 310-μm external diameter, molecular weight cutoff > 15 000 Da), prepared according to Ungerstedt,[27] was placed into the dorsal hippocampus and fixed with a screw and dental cement. Ringer solution (in mM: NaCl 122, KCl 3.1, $MgSO_4$ 1.2, KH_2PO_4 0.4, $CaCl_2$ 1.3, $NaHCO_3$ 25, glucose 10) perfused the probe at a rate of 2 μL/min. The animals were then placed in individual cages. The probe openings were closed. Twenty-four hours later the animals were once again connected to the perfusion apparatus. At least a 1-h stabilization was allowed before collecting the perfusates for KYNA determination.

Quantification of KYNA in Dialysate. KYNA was measured using HPLC with postcolumn derivatization and fluorescence detection.[3g] The dialysate was directly injected into the HPLC apparatus. A reversed-phase column (S 10 ODS2 Spherisorb) was used, and the separation was obtained using 50 mM sodium acetate buffer (pH 6.20) with 8% acetonitrile as mobile phase at a flow rate of 1.0 mL/min. The postcolumn derivatizing agent was zinc acetate (0.5 M) at a flow rate of 0.6 mL/min. The fluorimetric detection was performed with a Perkin-Elmer spectrophotofluorimeter LC 240 using an excitation wavelength of 344 nm and an emission of 398 nm.

Quantification of KYNA in Rat Tissue. Unanesthetized rats were decapitated, and their brains and other organs (liver, kidney, blood) were rapidly collected. After homogenization and purification on a Dowex exchange resin,[3e] the samples were injected into the HPLC apparatus and evaluated with the postcolumn derivatization method described above.

Quantification of KYN. KYN was measured in blood, tissue homogenates, or dialysis fluids by means of HPLC.[28] The dialysis fluids were injected directly into the HPLC apparatus, the tissues were homogenized in $HClO_4$ (0.4 N), and blood was mixed with an equal volume of $HClO_4$ (0.8 N). The mixtures were left to stand on ice for 15 min and then centrifuged at 10000*g* for 10 min; the supernatants were filtered and injected into the HPLC. The separation was achieved with a reversed-phase column (Spherisorb S10 ODS2) and a mobile phase containing 0.1 M ammonium acetate, 0.1 M acetic acid, and 2% acetonitrile. The absorbance was monitored at 365 nm using a UV detector Perkin-Elmer LC 90.

Quantification of 3-Hydroxykynurenine. 3-Hydroxykynurenine was separated and detected using a combination of HPLC and an electrochemical method[29] with minor modifications. The separation was obtained using a reversed-phase column (Spherisorb S10 ODS2) and a mobile phase consisting of 950 mL

of water, 20 mL of acetonitrile, 9 mL of triethylamine, 5.9 mL of phosphoric acid, 100 mg of sodium EDTA, and 1.8 g of heptanesulfonic acid at a flow rate of 1.5 mL/min. The detection was performed with a coulometric detector (ESA Coulochem 5100A) with preoxidation voltage of 0.03 V and an oxidation voltage of 0.23 V.

Quantification of Anthranilic Acid. Anthranilic acid was assessed by means of HPLC equipped with a fluorimetric detector. The separation was achieved with a reversed-phase column as above and a mobile phase constituted of sodium acetate buffer 20 mM containing 30% methanol. The detection was obtained with a Perkin-Elmer LC240 fluorimeter. The excitation wavelength was 312 nm and the emission 420 nm.

Convulsions. Maximal electroshock seizures were obtained in rats by delivering through corneal electrodes a train of stimuli having the following parameters: 300-ms total duration, 10-ms duration of each stimulus, 160-mA intensity, and 60-Hz frequency. The total duration of tonic and clonic convulsion was measured. Audiogenic convulsions were obtained in DBA-2 mice (22–25 days old, Charles River, Como, Italy) which were exposed to an electric bell generating a 110-dB sound for 60 s. Protection against such convulsions were defined as the absence of tonic or clonic seizures during exposure to the sound.

Evaluation of the Spontaneous Locomotor Activity. Rats treated with an intraperitoneal injection of saline or of different doses of *m*-NBA (**4b**) were evaluated for their spontaneous locomotor activity with an Animex activity meter. The number of interruptions of the photocells was monitored by individually placing the rats in clean cages for 20 min. Five rats were used at each dosage level.

References

(1) Kozikowski, A. P., Barrionuevo, G., Eds. *Neurobiology of NMDA receptor from chemistry to the clinic*; VHC Publishers Inc.: New York, 1991.

(2) For reviews see: (a) Stone, T. W.; Connick, J. H. Quinolinic acid and other kynurenines in the CNS. *Neuroscience* **1985**, *15*, 597–617. (b) Schwarcz, R. Metabolism and function of brain kynurenines. *Biochem. Soc. Trans.* **1993**, *21*, 77–82.

(3) (a) Perkins, M. N.; Stone, T. W. An iontophoretic investigation of the actions of convulsivant kynurenines and their interaction with the endogenous excitant quinolinic acid. *Brain Res.* **1982**, *247*, 184–187. (b) Stone, T. W.; Perkins, M. N. Actions of excitatory amino acids and kynurenic acid in the primate hippocampus: a preliminary study. *Neurosci. Lett.* **1984**, *52*, 335–340. (c) Foster, A. C.; Vezzani, A.; French, E. D.; Schwarcz, R. Kynurenic acid blocks neurotoxicity and seizures induced in rat by the related brain metabolite quinolinic acid. *Neurosci. Lett.* **1984**, *48*, 273–278. (d) Moroni, F.; Russi, P.; Lombardi, G.; Beni, M.; Carlà, V. Presence of kynurenic acid in the mammalian brain. *J. Neurochem.* **1988**, *51*, 177–180. (e) Moroni, F.; Pellegrini-Giampietro, D. E.; Alesiani, M.; Cherici, G.; Mori, F.; Galli, A. Glycine and kynurenate modulate the glutamate receptors present in the myenteric plexus and in cortical membranes. *Eur. J. Pharmacol.* **1989**, *163*, 123–126. (f) Kessler, M.; Terramani, T.; Lynch, G.; Baudry, M. A glycine site associated with N-methyl-D-aspartic acid receptors characterization and identification of a new class of antagonists. *J. Neurochem.* **1989**, *52*, 1319–1328. (g) Swartz, K. J.; During, M. J.; Freese, A.; Beal, M. F.; Cerebral synthesis and release of kynurenic acid: an endogenous antagonist of excitatory amino acids receptors. *J. Neurosci.* **1990**, *10*, 2965–2973.

(4) (a) Stone, T. W.; Perkins, M. N. Quinolinic acid: a potent endogenous excitant at amino acid receptors in rat CNS. *Eur. J. Pharmacol.* **1981**, *72*, 411–412. (b) Schwarcz, R.; Whetsell, W. O.; Mangano, R. M. Quinolinic acid: an endogenous metabolite that produces axonsparing lesions in rat brain. *Science* **1983**, *219*, 316–318. (c) Schwarcz, R.; Brush, G. S.; Foster, A. C.; French, A. D. Seizure activity and lesions after intrahippocampal quinolinic acid injection. *Expl. Neurol.* **1984**, *84*, 1–17. (d) Schwarcz, R.; Foster, A. C.; French, E. D.; Whetsell, W. O.; Köhler, C. Excitotoxic models for neurodegenerative disorders. *Life Sci.* **1984**, *35*, 19–32. (e) Beal, M. F.; Kowall, N. W.; Ellison, D. W.; Mazurek, M. F.; Swartz, K. J.; Martin, J. B. Replication of the neurochemical characteristics of Huntington's disease by quinolinic acid. *Nature* **1986**, *321*, 168–171. (f) Heyes, M. P. Hypothesis: a role for quinolinic acid in the neuropathology of glutaric aciduria type I. *Can. J. Neurol. Sci.* **1987**, *14*, 441–443. (g) Speciale, C.; Okuno, E.; Schwarcz, R. Increased quinolinic acid metabolism following neuronal degeneration in the rat hippocampus. *Brain Res.* **1987**, *436*, 18–24. (h) Schwarcz, R.; Tamminga, C. A.; Kurlan, R.; Shoulson, I. Cerebrospinal fluid levels of quinolinic acid in Huntington's disease and schizophrenia. *Ann. Neurol.* **1988**, *24*, 580–582. (i) Heyes, M. P.; Swartz, K. J.; Markey, S. P.; Beal, M. F. Regional brain and cerebrospinal fluid quinolinic acid concentrations in Huntington's disease. *Neurosci. Lett.* **1991**, *122*, 265–269. (j) Heyes, M. P.; Brew, B. J.; Martin, A.; Price, R. W.; Salazar, A. M.; Sidtis, J. J.; Yergey, J. A.; Mouradian, M. M.; Sadler, A. E.; Keilp, J.; Rubinow, D.; Markey, S. P. Quinolinic acid in cerebrospinal fluid and serum in HIV-1 infection: relationship to clinical and neurological status. *Ann. Neurol.* **1991**, *29*, 202–209.

(5) Saito, K.; Nowak, T. S., Jr.; Markey, S. P.; Heyes, M. P. Mechanism of delayed increases in kynurenine pathway metabolism in damaged brain regions following transient cerebral ischemia. *J. Neurochem.* **1993**, *60*, 180–192.

(6) (a) Moroni, F.; Alesiani, M.; Facci, L.; Fadda, E.; Skaper, S. D.; Galli, A.; Lombardi, G.; Mori, F.; Ciuffi, M.; Natalini, B.; Pellicciari, R. Thiokynurenates prevent excitotoxic neuronal death in vitro and in vivo by acting as glycine antagonists and as inhibitors of lipid peroxidation. *Eur. J. Pharmacol.* **1992**, *218*, 145–151. (b) Carling, R. W.; Leeson, P. D.; Moseley, A. M.; Baker, R.; Foster, A. C.; Grimwood, S.; Kemp, J. A.; Marshall, G. R. 2-Carboxytetrahydroquinolines. Conformational and stereochemical requirements for antagonism of the glycine site on the NMDA receptor. *J. Med. Chem.* **1992**, *35*, 1942–1953 and references therein.

(7) Bender, D. A. Biochemistry of tryptophan in health and disease. *Mol. Aspects Med.* **1982**, *6*, 101–197.

(8) Fukui, S.; Schwarz, R.; Rapoport, S. I.; Takada, Y.; Smith, Q. R. Blood-brain barrier transport of kynurenines: implications for brain synthesis and metabolism. *J. Neurochem.* **1991**, *56*, 2007–2017.

(9) Gal, E. M.; Sherman, A. D. Synthesis and metabolism of L-kynurenine in rat brain. *J. Neurochem.* **1978**, *30*, 607–613.

(10) (a) Turski, W. A.; Gramsbergen, J. B. P.; Traitler, H.; Schwarcz, R. Rat brain slices produce and liberate kynurenic acid upon exposure to L-kynurenine. *J. Neurochem.* **1988**, *71*, 563–567. (b) Speciale, C.; Hares, K.; Schwarcz, R.; Brookes, N. High affinity uptake of L-kynurenine by a sodium-independent transporter of neutral amino acids in astrocytes. *J. Neurosci.* **1989**, *9*, 2066–2072.

(11) (a) Speciale, C.; Schwarcz, R. Uptake of kynurenine into rat brain slices. *J. Neurochem.* **1990**, *54*, 156–163. (b) Heyes, M. P.; Quearry, B. J. Quantification of kynurenic acid in cerebrospinal fluid: effects of systemic and central L-kynurenine administration. *J. Chromatogr.* **1990**, *530*, 108–112.

(12) Speciale, C.; Ungerstedt, U.; Schwarcz, R. Production of extracellular quinolinic acid in the striatum studied by microdialysis in unanesthetized rats. *Neurosci. Lett.* **1989**, *104*, 345–350.

(13) Turski, W. A.; Nakamura, M.; Todd, W. P.; Carpenter, B. K.; Whetsell, W. O., Jr.; Schwarcz, R. Identification and quantification of kynurenic acid in human brain tissue. *Brain. Res.* **1988**, *454*, 164–169.

(14) (a) Vecsei, L.; Miller, J.; Macgarvey, U.; Beal, M. F. Kynurenine and probenecid inhibit pentylenetetrazol and NMDA induced seizures and increase kynurenic acid concentration in the brain. *Brain. Res. Bull.* **1992**, *28*, 233–238. (b) Nozaki, K.; Beal, M. F. Neuroprotective effects of L-kynurenine on hypoxia/ischemia and NMDA lesions in neonatal rats. *J. Cereb. Blood Flow Metab.* **1992**, *12*, 400–407.

(15) Cady, S. G.; Sano, M. 1-Methyl-DL-tryptophan, β-(3-benzofuranyl)-DL-alanine (the oxygen analog of tryptophan) are competitive inhibitors for indoleamine-2,3-dioxygenase. *Arch. Biochem. Biophys.* **1991**, *291*, 326–333 and references therein.

(16) Dua, K. R.; Taylor, E. W.; Phillips, R. S. S-aryl-L-cysteine S,S-dioxides: design, synthesis, and evaluation of a new class of inhibitors of kynureninase. *J. Am. Chem. Soc.* **1993**, *115*, 1264–1270.

(17) (a) Moroni, F.; Russi, P.; Gallo-Mezo, M. A.; Moneti, G.; Pellicciari, R. Modulation of quinolinic and kynurenic acid content in the rat brain: effect of endotoxins and nicotinylalanine. *J. Neurochem.* **1991**, *57*, 1630–1635. (b) Russi, P.; Alesiani, M.; Lombardi, G.; Davolio, P.; Pellicciari, R.; Moroni, F. Nicotinylalanine increases the formation of kynurenic acid in the brain and antagonizes convulsions. *J. Neurochem.* **1992**, *59*, 2076–2080. (c) Pellicciari, R.; Gallo-Mezo, M. A.; Natalini, B.; Amer, A. M. Stereospecific synthesis of the enantiomers of nicotinylalanine, a neuroprotecting agent. *Tetrahedron Lett.* **1992**, *33* (21), 3003–3004. See also: (d) Connick, J. H.; Heywood, G. C.; Sill, G. J.; Thompson, G. G.; Brodie, M. J.; Stone, T. W. Nicotinylalanine increases cerebral kynurenic acid content and has anticonvulsivant activity. *Gen. Pharmacol.* **1992**, *23*, 235–239.

(18) Shibata, Y. On the regulation of tryptophan metabolism "via" kynurenine. *Acta Vitaminol. Enzymol.* **1978**, *32*, 195–207.

(19) (a) Saito, Y.; Hayaishi, O.; Rothberg, S. Enzymic formation of 3-hydroxy-L-kynurenine from L-kynurenine. *J. Biol. Chem.* **1957**, *229*, 921–933. (b) Okamoto, H.; Hayaishi, O. FAD requirement for kynurenine hydroxylase of rat liver mitochondria. *Biochem. Biophys. Res. Commun.* **1967**, *29*, 394–399. (c) Nisimoto, Y.; Tacheuchi, F.; Shibata, Y. Molecular properties of L-kynurenine-3-hydroxylase from rat liver mitochondria. *J. Biochem.* **1977**, *81*, 1413–1425. (d) Bender, D. A.; McCreanor, G. M. Kynurenine hydroxylase: a potential rate-limiting enzyme in tryptophan metabolism. *Biochem. Soc. Trans.* **1985**, *13*, 441–443. (e) Wiseman, J. S.; Nichols, J. S. A radiometric kynurenine monoxygenase assay. *Anal. Biochem.* **1990**, *184*, 55–58.

(20) Nishimoto, Y.; Takeucki, F.; Shibata, Y. Purification of L-kynurenine-3-hydroxylase by affinity chromatography. *J. Chromatogr.* **1979**, *169*, 357–364.
(21) (a) Wessiak, A.; Schopfer, L. M.; Massey, V. pH Dependence of the reoxydation of *p*-hydroxybenzoate hydroxylase·2,4-hydroxybenzoate complex. *J. Biol. Chem.* **1984**, *259*, 12547–12556. (b) Müller, F. Flavin-dependent hydroxylases. *Biochem. Soc. Trans.* **1985**, *13*, 443–447.
(22) Entsch, B.; Ballou, D. P.; Massey, V. Flavin oxygen derivatives involved in hydroxylation by *p*-hydroxybenzoate hydroxylases. *J. Biol. Chem.* **1976**, *251*, 2550–2563.
(23) Snyder, J. P.; Rao, S. N.; Koehler, K. F.; Pellicciari, R. Drug modeling at cell membrane receptors. The concept of pseudoreceptor. In *Trends in Receptor Research*; Angeli, P., Gulini, U., Quaglia, W., Eds.; Elsevier: Amsterdam, 1992; pp 367–403.
(24) Snyder, J. P.; Rao, S. N.; Pellicciari, R.; Monahan, J. B. Receptor modeling of highly charged excitatory amino acids using the molecular dynamics/free energy perturbation approach. In *Frontiers in Drug Research: Crystallographic and Computational Methods*; Jensen, B., Jørgensen, F. S., Kofod, H., Eds.; Munksgaard: Copenhagen, 1990; pp 109–118.
(25) Goodford, P. J. A computational procedure for determining energetically favorable binding sites on biologically important macromolecules. *J. Med. Chem.* **1985**, *28*, 849–857.
(26) Stewart, J. J. P. Optimization of parameters for semiempirical methods. I. Method. *J. Comput. Chem.* **1989**, *10*, 209–220.
(27) Ungerstedt, U. Measurement of neurotransmitter release by intracranial dialysis. In *Measurement of Transmitter Release*; Marsden, C. A., Ed.; John Wiley: Chichester, 1984; pp 81–105.
(28) Holmes, E. W. Determination of serum kynurenine and hepatic tryptophan dioxygenase activity by HPLC. *Anal. Biochem.* **1988**, *172*, 518–525.
(29) Heyes, M. P.; Quearry, B. J. Quantification of 3-hydroxy-kynurenine in the brain by high-performance liquid chromatography and electrochemical detection. *J. Chromatogr.* **1988**, *428*, 340–344.
(30) Tallarida, R. J.; Murray, R. B. *Manual of Pharmacological correlations with computer programs*, 2nd ed.; Springer Verlag: New York, 1987.